



ELSEVIER



ScienceDirect

Ocean Modelling xxx (2007) xxx–xxx

**Ocean  
Modelling**[www.elsevier.com/locate/ocemod](http://www.elsevier.com/locate/ocemod)

## Sensitivity of wind waves to hurricane wind characteristics

Huiqing Liu<sup>a</sup>, Lian Xie<sup>a,\*</sup>, Leonard J. Pietrafesa<sup>b</sup>, Shaowu Bao<sup>a</sup><sup>a</sup> *Department of Marine, Earth and Atmospheric Sciences, North Carolina State University, Box 8208, Raleigh, NC 27695-8208, United States*<sup>b</sup> *College of Physical and Mathematical Sciences, North Carolina State University, Raleigh, NC, United States*

Received 4 October 2006; received in revised form 6 March 2007; accepted 7 March 2007

### Abstract

In this study, the influence of the spatial and temporal variability of hurricane winds, storm translation speed, intensity, and ambient wind field on surface wind waves are investigated by using a third-generation wave model (Simulating WAVes Nearshore, or SWAN). The results show that the asymmetric structure of wind-induced wave field is sensitive not only to the asymmetric structure of the hurricane wind field, but also to the variations in the storm translation speed and intensity. The significant wave height (SWH) in the front-right quadrant of the storm rises as storm translation speed increases until it reaches a critical value, then the SWH drops. The opposite occurs in the rear-left quadrant. The total contribution of the hurricane translation speed to the asymmetric structure of the wave field also depends on the intensity of the hurricane. As the intensity of the hurricane increases, the relative significance of the influence of the translation speed on the asymmetric structure of the wave field decreases. Most parametric hurricane wind models can only model symmetric hurricanes and do not include background winds. However, actual hurricanes in nature are not only asymmetric but also imbedded in background winds. Thus, to more properly model hurricane-induced wave field, it is important to consider storm asymmetry, translation speed, intensity, as well as background winds.

© 2007 Published by Elsevier Ltd.

*Keywords:* Wave; Hurricane; Numerical modeling; Ocean response; Wind forcing

### 1. Introduction

Waves generated by hurricanes can exceed 20 m in deep open ocean waters. Wang et al. (2005) reported that the maximum significant wave height (SWH) reached 27.7 m during the passage of Hurricane Ivan. Although SWH is lower when waves reach shallow waters, these waves can devastate the coastal zone. It is well known that hurricane-induced waves are one of the most damaging phenomena during the passages of hurricanes. Severe wave conditions are dangerous to vessels in ocean and coastal waters, and waves can also run up over the storm surge in the coastal zone to cause more severe damage along and on the coast. So the ability to predict hurricane-induced waves precisely is a very important challenge and is of great value to many

\* Corresponding author. Tel.: +1 919 5151435; fax: +1 919 5157802.

E-mail address: [xie@ncsu.edu](mailto:xie@ncsu.edu) (L. Xie).

33 user communities. As the wind is the principal source of energy creating and driving waves, in order to forecast  
 34 hurricane-induced ocean surface waves, it is necessary to establish a thorough understanding of how the wave  
 35 field manifests itself in response to the spatial and temporal variation of hurricane winds.

36 During the 1950s, the resonance mechanism (Phillips, 1957) and the feed-back mechanism (Miles, 1957) of  
 37 how wind energy is transferred to waves were developed. Most of the present community wave models (e.g.,  
 38 WAM by the WAMDI, 1988; and SWAN by Booij et al., 1999) still use the concepts introduced by the pio-  
 39 neering works of Phillips and Miles as the mechanisms of wind energy input into ocean surface waves. These  
 40 two wave models have been verified and used to forecast waves, hind-cast waves and in wave-current inter-  
 41 action analyses in many oceans around the world (WAMDI, 1988; Komen et al., 1994; Xie et al., 2001; Booij  
 42 et al., 1999; Ris et al., 1999).

43 There have been a number of past studies on the response of wind waves to tropical cyclones including data  
 44 analysis and numeric model studies. Wright et al. (2001) and Walsh et al. (2002) provided all quadrants of sea  
 45 surface directional wave spectrum in the open water (August 24, 1998) and at landfall (August 26, 1998) during  
 46 hurricane Bonnie using the NASA airborne scanning radar altimeter data. They found that the dominant waves  
 47 generally propagated at significant angles to the downwind direction, and developed a simple model to predict  
 48 the dominant wave propagation direction. Recently, Young (2006) studied the directional wave spectrum dur-  
 49 ing the passages of several hurricanes using wave buoy observations and showed that in almost all quadrants of  
 50 the storm, the dominant waves are remotely generated swells. In the meantime, Ou et al. (2002) used SWAN to  
 51 simulate typhoon-induced waves in the coastal waters of Taiwan. Their results showed that waves under  
 52 typhoon forcing condition can be reasonably well simulated by the SWAN wave model. Moon et al. (2003) sim-  
 53 ulated the surface wave spectra under hurricane wind forcing using a high resolution WAVEWATCH III model  
 54 (Tolman, 1991). They showed that numerical simulation results agree reasonably well with observational data.  
 55 Furthermore, they also analyzed the effect of hurricane translation speed on the wave spectra. However, their  
 56 study focused on the analysis of a specific case. Moon et al. (2004) investigated the effect of sea surface waves on  
 57 air–sea momentum flux during the passages of tropical cyclones. A remaining issue which has received little  
 58 attention in the past is the sensitivity of surface wind waves to the spatial and temporal variations of tropical  
 59 cyclone winds. In order to address this issue, a suite of numerical experiments are designed to quantify the influ-  
 60 ence of wind distribution, storm translation speed and intensity on ocean surface wind waves using SWAN.  
 61 Additionally, two historical hurricane cases (Hurricane Bonnie, 1998 and Floyd, 1999) are studied to quantify  
 62 the effects of actual hurricane structure and background wind field on waves. A brief description of the SWAN  
 63 model and parameteric hurricane wind models are given in Section 2. Section 3 describes the model experi-  
 64 ments. Results are presented in Section 4, followed by discussions and conclusions.

## 65 2. Model description

### 66 2.1. The SWAN wave model

67 The SWAN model is based on the wave action balance equation (or energy balance in the absence of cur-  
 68 rents) with sources and sinks. In SWAN the evolution of the wave spectrum is described by the spectral action  
 69 balance equation, which for Cartesian coordinates (e.g., Hasselmann et al., 1973) is:

$$71 \quad \frac{\partial}{\partial t} N + \frac{\partial}{\partial x} C_x N + \frac{\partial}{\partial y} C_y N + \frac{\partial}{\partial \sigma} C_\sigma N + \frac{\partial}{\partial \theta} C_\theta N = \frac{S}{\sigma} \quad (1)$$

72 where  $N$  is the wave action density ( $N(\sigma, \theta) = E(\sigma, \theta)/\sigma$ ),  $E$  is the energy density spectrum,  $\sigma$  is the relative frequency  
 73 and  $\theta$  is wave propagation direction.  $X$  and  $Y$  are Cartesian coordinates.  $C_x$ ,  $C_y$ ,  $C_\sigma$  and  $C_\theta$  are wave prop-  
 74 agation speeds in  $x$ -,  $y$ -,  $\sigma$ - and  $\theta$ -space, respectively.  $S$  is the source term which represents the effects of gen-  
 75 eration, dissipation and nonlinear wave–wave interactions.

### 76 2.2. Hurricane wind models

77 Two hurricane wind models are employed in this study to simulate hurricane winds, one is the symmetric  
 78 Holland (1980) model (hereafter referred to as H1980) and the other is an asymmetric Holland–NCSU model

79 (Xie et al., 2006) (referred to as HN2006 hereafter). In H1980, the wind speed as a function of radial distance  
80 from the center of the storm is described as

$$83 \quad V_a = [AB(P_n - P_c) \exp(-A/r^B) / \rho_a r^B]^{1/2} \quad (2)$$

84 where  $V_a$  is wind speed at radius  $r$ ,  $P_c$  is the central pressure,  $P_n$  is the ambient pressure ( $P_n$  is set to 1000 mb in  
85 this study), and  $A$ ,  $B$  are scaling parameters ( $A = (R_{\max})^B$ ) in which  $R_{\max}$  is the radius of maximum wind  
86 (RMW). Wind field parameters used in Eq. (2) were obtained from the National Hurricane Center (NHC)  
87 of the United States National Oceanic and Atmospheric Administration (NOAA).

88 In the comparison experiment, the hurricane wind field is obtained by combining an asymmetric hurricane  
89 wind field produced by HN2006 with the background wind field. In the asymmetric hurricane wind model,  
90  $R_{\max}$  in Eq. (2) was modified to fit a polynomial function of the azimuthal angle  $\theta$ :

$$92 \quad R_{\max}(\theta) = P_1 \theta^{n-1} + P_2 \theta^{n-2} + \dots + P_{n-1} \theta + P_n \quad (3)$$

93  $B$  and  $R_{\max}$  in Eq. (2) are then optimized using available observational data, wind analysis or forecast guid-  
94 ance. The background wind field was obtained by removing the hurricane vortexes in the eta data assimilation  
95 system (EDAS) data, which are often coarse and weak, using a cylindrical filtering operator (Kurihara et al.,  
96 1993). Then the optimized asymmetric hurricane wind field described above was imbedded into the back-  
97 ground wind field to produce the total wind field.

### 98 3. Experimental designs

99 Four experiments are designed to investigate the effect of Hurricane translation speed, intensity and struc-  
100 ture on the wave field. The experiments are listed in Table 1. Hurricane wind fields for these experiments are  
101 simulated by H1980 for symmetric wind cases and by HN2006 for the asymmetric hurricane cases as well as  
102 for Hurricane Bonnie in 1998 and Floyd in 1999. For the symmetric hurricane experiments, an idealized  
103 domain and bathymetry are assumed, which is 1500 km in the  $x$ -direction and 3000 km in the  $y$ -direction.  
104 The water depth is set to a constant 5000 m for convenience. The moving direction of the hurricanes is from  
105 south to north. In these experiments, the wind field is translated across the model domain along the storm  
106 track and after the wave model is initiated with a “cold start” from a quiescent sea state. The first 75 h of  
107 the simulation was considered as a “spin-up” and the data after 75 h are analyzed. The settings for the asym-  
108 metric hurricane experiments will be presented in Section 4.4.

109 In Exp. A, 15 hurricane cases are used to study the effect of the hurricane translation speed on waves. All 15  
110 hurricanes have the same intensity (identical central pressure) but travel at different translation speeds. The  
111 effect of hurricane intensity on waves is investigated in Exp. B, as the hurricane translation speed is set to  
112 0 and different central pressures are assumed. Next, the combined effects of hurricane intensity and translation  
113 speeds on waves are examined in Exp. C. Finally, the effects of hurricane wind structure and background wind  
114 field on waves are investigated in Exp. D, which includes real hurricane cases of Hurricane Bonnie (1998) and  
115 Floyd (1999). The observed hurricane translation speed and center pressure are used in these two cases. Hur-  
116 ricanes in Exps. A, B and C have the same RMW.

## 117 4. Results

### 118 4.1. The effect of hurricane translation speed on waves

119 The distributions of SWH, relative to the hurricane center and driven by symmetric hurricanes with differ-  
120 ent translation speeds (Exp. A) are shown in Fig. 1. Fig. 1 also displays the SWH differences between each case  
121 and the SWH generated by a static hurricane. These SWHs are plotted at locations within a distance of  
122 300 km from the center of the hurricane. Fig. 1 shows that the SWH in the front-right quadrant of the storm  
123 track increases, while that in the rear-left quadrant decreases, with increasing hurricane translation speed.  
124 This result is consistent with the findings of Moon et al. (2004). The results indicate that hurricane translation  
125 speed can cause asymmetric distribution of waves regardless of whether the hurricane is symmetric or  
126 asymmetric.

Table 1  
Experimental designs

| Exp. name | Hurricane Translation speed (m/s) | Center pressure (intensity)(hpa) | Structure         |                         |
|-----------|-----------------------------------|----------------------------------|-------------------|-------------------------|
| A         | From 0 to 14<br>Interval = 1 m/s  | 963                              | Symmetric         |                         |
| B         | 0                                 | 953<br>963<br>973                | Symmetric         |                         |
| C         | C1                                | 0                                | 953<br>963<br>973 | Symmetric               |
|           |                                   | C2                               | 1                 |                         |
|           | C3                                |                                  | 2                 |                         |
|           |                                   | C4                               | 3                 |                         |
|           | C5                                |                                  | 4                 |                         |
|           |                                   | C6                               | 5                 |                         |
| D         | Varying                           |                                  | Varying           | Symmetric<br>Asymmetric |

127 It is worth noting that, initially the hurricane translation speed increases from 0 to approximately 12 m/s,  
 128 the SWH in the front-right quadrant of the storm track also increases, but when the translation speed exceeds  
 129 13 m/s, the SWH begins to decrease. To illustrate this trend, the SWH values of the waves generated by hur-  
 130 ricanes moving with different translation speeds at a location in the first quadrant and one RMW away from  
 131 the storm center (Point A in Fig. 2), and a location in the third quadrant, which is also one RMW away from  
 132 the storm center (Point B in Fig. 2), are plotted in Fig. 3. Note that Point A is located at 45° angle (front-  
 133 right), while Point B is 235° angle (rear-left) to the storm motion. It can be seen that the SWH at Point A  
 134 monotonically increases with the translation speed from 0 to 12 m/s, but begins to drop when the translation  
 135 speed exceeds 13 m/s. This phenomenon can be explained by the following resonance theory proposed by King  
 136 and Shemdin (1978) and elaborated by others (Young, 1988; Bowyer and MacAfee, 2000; Moon et al., 2003):  
 137 “waves to the right of the hurricane track are exposed to the prolonged forcing of winds, and as the hurricane  
 138 translation speed becomes comparable to the group speed of the dominant waves, those waves essentially  
 139 become trapped within the hurricane and there appears to be resonance between swells produced previously  
 140 by the hurricane and the locally generated wind waves.” The period of the dominant wave generated by this  
 141 intense hurricane is 15.89 s and the corresponding group velocity of the dominant wave is 12.3 m/s. Fig. 4  
 142 shows the one dimensional directional wave spectrum at Point A. It can also be seen from Fig. 4a–g that wave  
 143 energy increases with increasing translation speed. However, it shows the presence of only one spectrum  
 144 energy peak, which is located near 100°, because the direction of swells (Fig. 6) is similar to the direction  
 145 of local wind-generated waves at Point A. The notion that waves in the forward quadrants of storm are being  
 146 dominated by swell is also verified by observational data (Wright et al., 2001; Young, 2006). In contrast, as the  
 147 hurricane translation speed becomes greater than the group speed of the dominant waves, the waves to the  
 148 right of the hurricane track are less likely to be trapped within the influence of the hurricane. Hence, previ-  
 149 ously generated swells at Point A will not have the opportunity to interact with new waves generated by

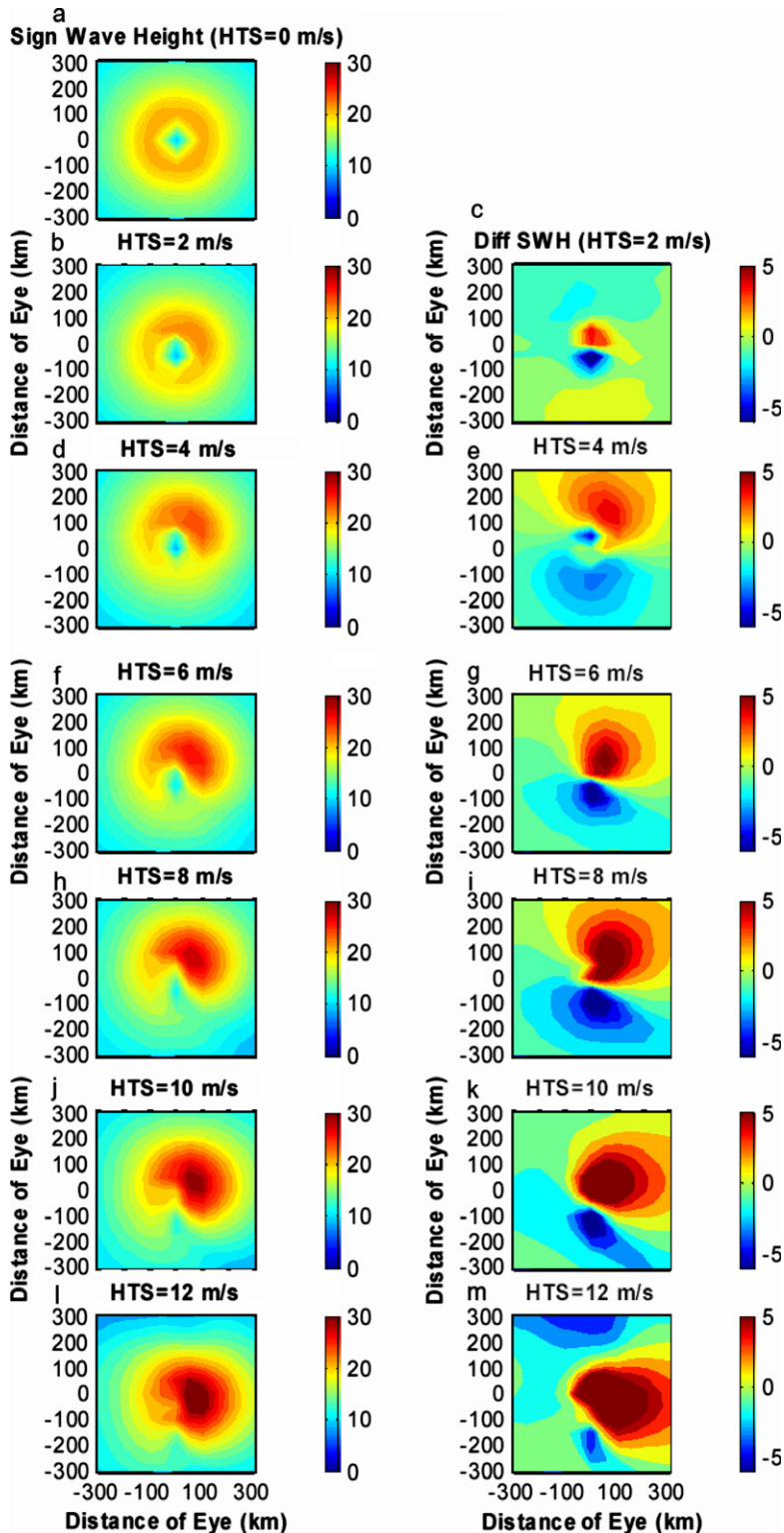


Fig. 1. The distribution of significant wave height (SWH) driven by static symmetric hurricanes (a) and symmetric hurricanes with different translation speeds (b) 2 m/s; (d) 4 m/s; (f) 6 m/s; (h) 8 m/s; (j) 10 m/s; (l) 12 m/s and different SWH differences between them and these generated by the static hurricane (c) 2 m/s; (e) 4 m/s; (g) 6 m/s; (i) 8 m/s; (k) 10 m/s; (m) 12 m/s.

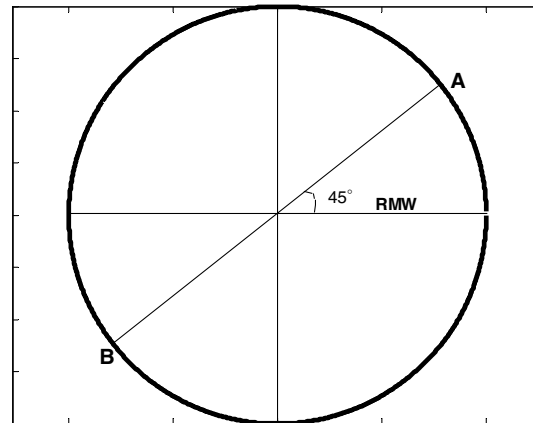


Fig. 2. The locations of two sampling points. Point 'A' locates in the first quadrant one RMW from the storm center, while point 'B' locates in the third quadrant, also one RMW away from the storm center.

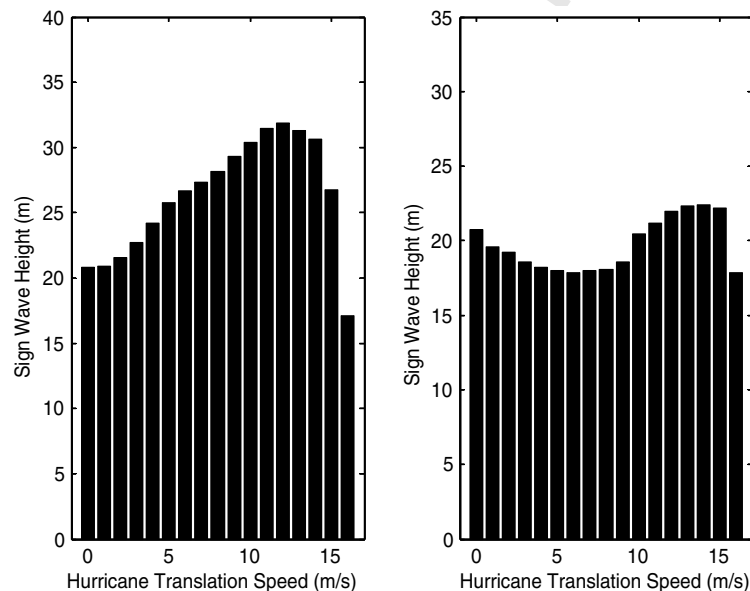


Fig. 3. SWH values of waves generated by symmetric hurricanes moving with different translation speeds of location 'A' (a) and location 'B' (b) (shown in Fig. 2) at RMWs.

150 the hurricane. In other words, there is no resonance effect at the front-right quadrant of the hurricane, and as a  
 151 result, wave energy starts to decrease at Point A because of the reduction of the duration of wind action  
 152 (Fig. 4h).

153 The situation at Point B is the opposite. At the beginning, the SWH at the rear-left of the hurricane  
 154 decreases monotonically with increasing hurricane translation speed (Fig. 3b). However, it starts to increase  
 155 when the translation speed reaches about 7 m/s and its maximum value occurs at 15 m/s. Furthermore, the  
 156 SWH at Point B generated by the hurricane with a translation speed at (or in excess of) 11 m/s will be higher  
 157 than that induced by a static hurricane (Fig. 3b). Fig. 5 shows the one dimensional directional wave spectrum  
 158 at Point B. It can be seen from Fig. 5a–d that the major wave spectrum energy is located between 270° and  
 159 360°, which is the same as the local wind direction. In other words, SWH is mainly contributed from locally-

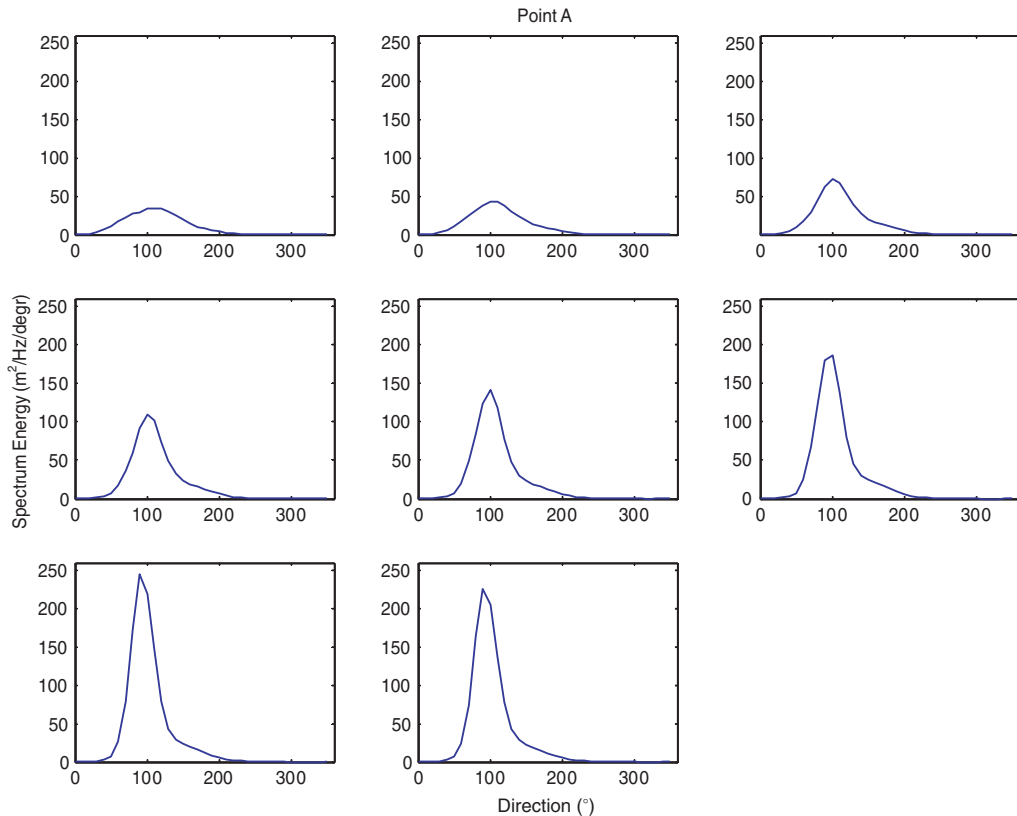


Fig. 4. One dimensional directional wave spectrum at Point A, which were generated by symmetric hurricanes moving with different translation speeds: (a) 0 m/s; (b) 2 m/s; (c) 4 m/s; (d) 6 m/s; (e) 8 m/s; (f) 10 m/s; (g) 12 m/s and (h) 14 m/s.

160 generated wind waves because the waves are not trapped when the storm translation speed is below the group  
 161 speed of the dominant waves. Therefore, SWH of locally-generated wind waves are reduced at the beginning  
 162 (Fig. 5a–d) due to reduced forcing time as the waves propagate against the hurricane moving direction. How-  
 163 ever, with increasing translation speed, it becomes possible for waves generated on the right side of the track  
 164 under “near-resonance” conditions to reach Point B, as will be discussed later. This is also due to the re-  
 165 sponse between the swells and the locally generated wind waves. It can be explained by using Fig. 5e–h. There  
 166 is another peak in the spectral energy distribution located between 100° and 140°. It is obvious that this energy  
 167 peak does not correspond to waves generated by local winds, but from swells transported from some distance.  
 168 The SWH at Point B increases until the hurricane translation speed increases to a critical value 15 m/s in the  
 169 case considered here. Same as at Point A, SWH at Point B decreases as the storm translation speed increases  
 170 beyond this critical value and the duration of wind action reduces with the increase of hurricane translation  
 171 speed.

172 The reason why the two critical values of storm translation speed at Point A and Point B are different can  
 173 be explained by using Fig. 6, which shows a schematic picture of swell (of Point A and Point B) propagating in  
 174 the direction tangential to the circle defined by the RMW at an earlier position of the storm. This schematic  
 175 picture is based on the assumption that the swell is generated from the earlier position of the storm and the  
 176 propagation direction of the swell at each point is determined by the waves propagating in the direction tan-  
 177 gential to circle of RMW at the earlier position of the storm (Fig. 6) (Moon et al., 2003). The maximum SWH  
 178 is achieved for swells that maximize their forcing time under the hurricane, which (at least approximately) cor-  
 179 responds to having the component of swell propagation velocity in the translation direction equal to the hur-  
 180 ricane translation speed. Given the angle needed for waves to reach Point B, as shown in Fig. 6, this requires a  
 181 greater hurricane translation speed for Point B than for Point A.

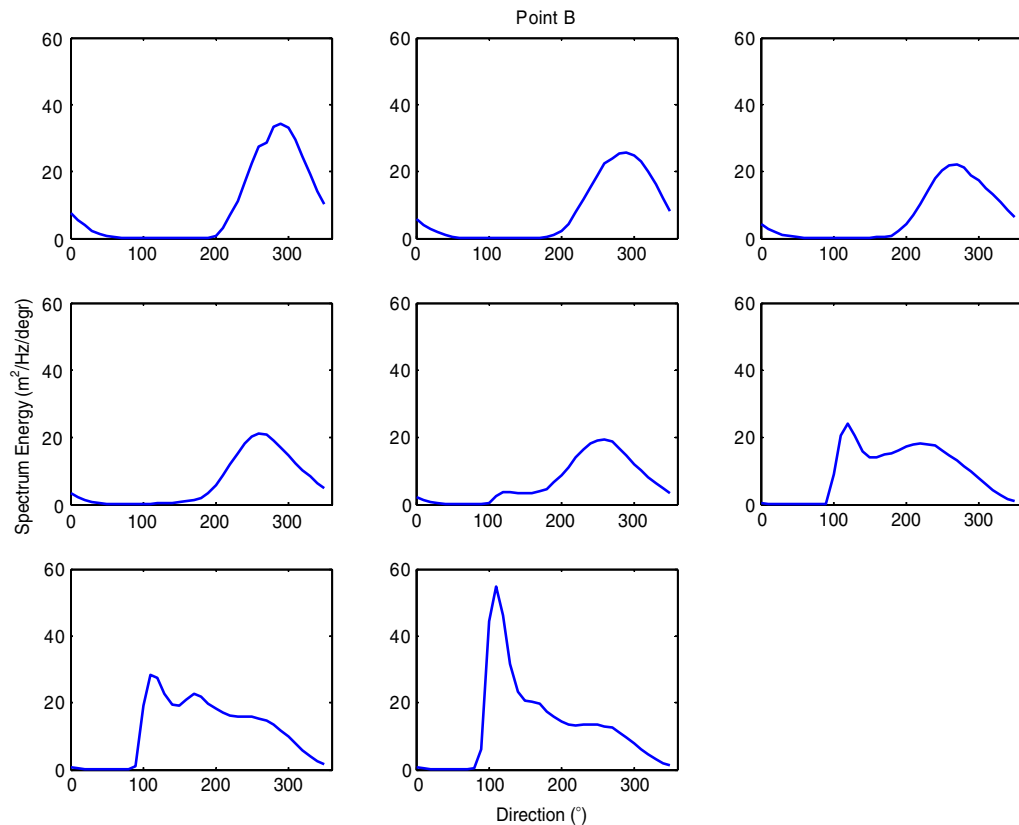


Fig. 5. Same as Fig. 4 except for Point B.

#### 182 4.2. The effect of hurricane intensity on waves

183 In Exp. B, three static hurricanes with different center pressure (intensity) were used to investigate the effect  
 184 of hurricane intensity on waves. One is a strong hurricane whose central pressure is 953 hpa (maximum wind  
 185 velocity, MWV is 44 m/s), the second is a moderate hurricane whose central pressure is 963 hpa  
 186 (MWV = 39 m/s) and the third is a weak hurricane whose central pressure is 973 hpa (MWV = 34 m/s).  
 187 The SWH at locations A and B, as indicated in Fig. 2, is shown in Fig. 7 for the three different hurricane cases.  
 188 It is obvious that the SWH at the two points indicated in Fig. 2 increases with hurricane intensity, but the  
 189 intensity of the hurricane does not affect the asymmetric structure of waves.

190 The question is what would the combined effects of hurricane intensity and translation speed be on the  
 191 SWH of the wave field? This question will be addressed in the next section.

#### 192 4.3. The effect of the combined hurricane intensity and translation speed on waves

193 In this section, we will examine how waves vary with varying hurricane intensity and translation speed. Dif-  
 194 ferent hurricanes with translation speeds at 0, 1, 2, 3, 4 and 5 (m/s), each of which has different central pres-  
 195 sures, were used in Exp. C (Table 1). We will examine whether or not the effect of the hurricane translation  
 196 speed on waves depends on hurricane intensity. The normalized SWH difference (NSD) between C2 (C3, C4,  
 197 C5 or C6) and C1 at locations A and B is defined as

$$199 \quad \text{NSD} = \frac{\text{SWH}_{C_i} - \text{SWH}_{C_1}}{\text{SWH}_{C_1}} \times 100\%$$



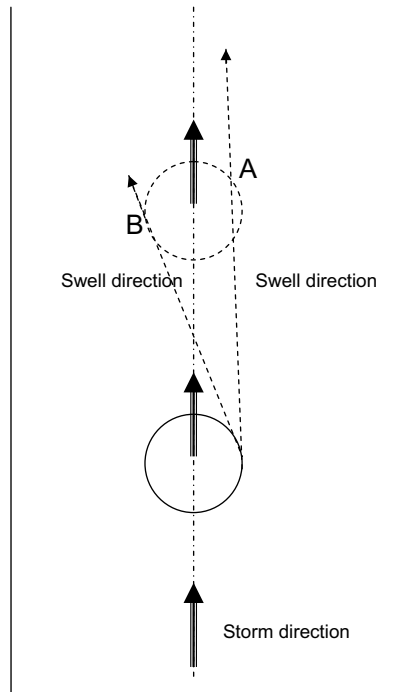


Fig. 6. Schematic picture of swell (of Point A and Point B) propagating in the direction tangential to the circle defined by the RMW at an earlier position of the storm.

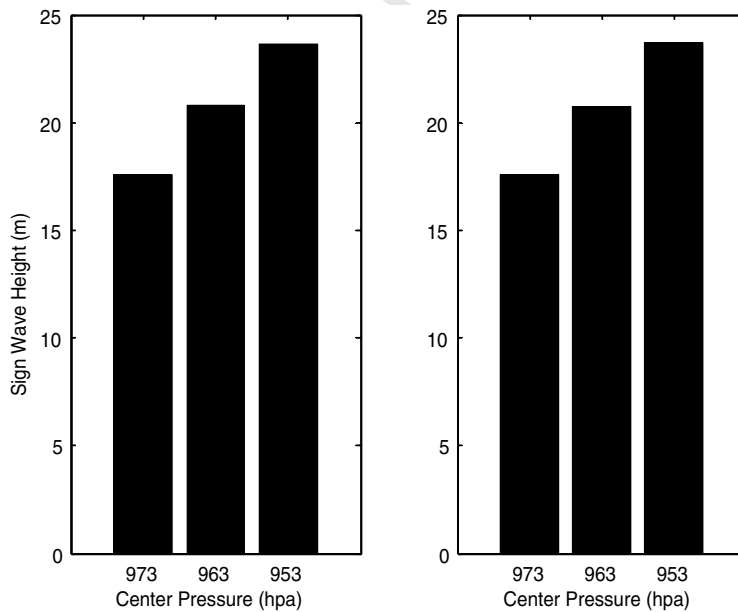


Fig. 7. SWH values of waves generated by static and symmetric hurricanes with different intensity of location 'A' (a) and location 'B' (b) (shown in Fig. 2) at RMWs.

200 It was used to represent the impact of hurricane translation speed on waves where  $SWH_{C_i}$  represents the  
 201 SWH in Exps. C2, C3 C4, C5 or C6, and  $SWH_{C1}$  represents the SWH in Exp. C1. Fig. 8 shows that the  
 202 NSD at locations A and B (as shown in Fig. 2) varies with different intensity and translation speed. It is obvi-

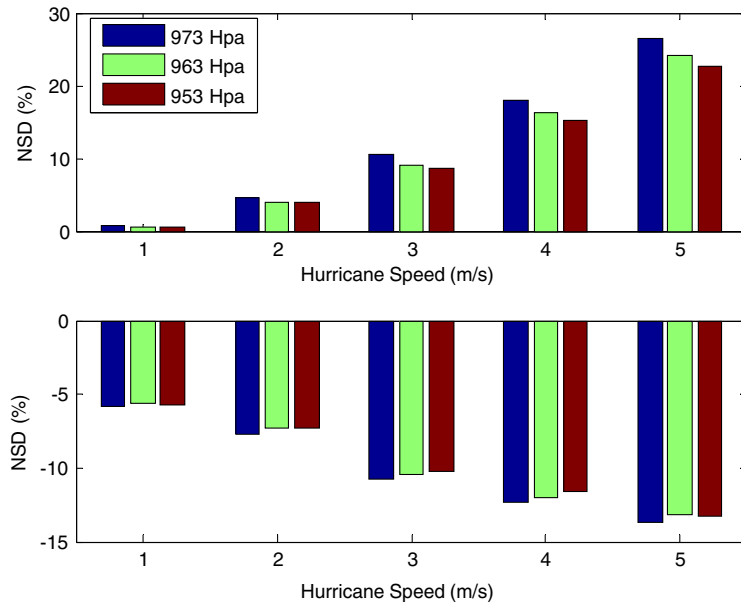


Fig. 8. Normalized SWH difference (NSD) at location 'A' (a) and location 'B' (b) (shown in Fig. 2).

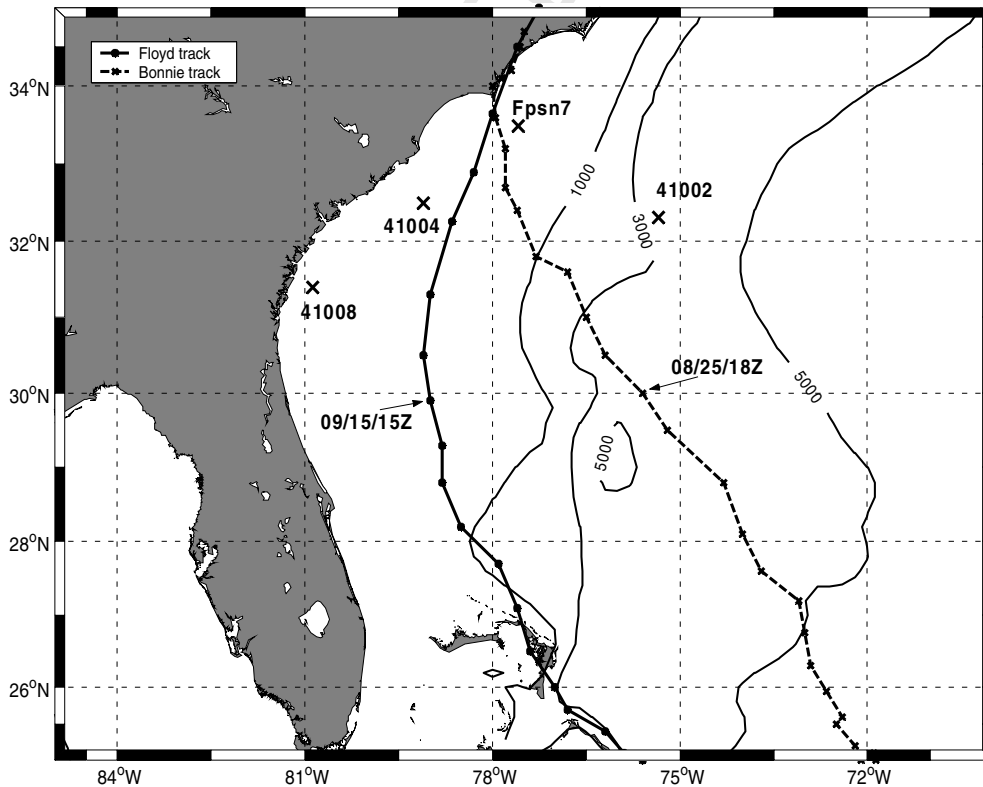


Fig. 9. The model topography and domain used in experiment D, extends latitudinally from 25° to 35° north and longitudinally from 85° to 70° west. Dashed-X line and solid-point line are the best tracks of Bonnie and Floyd respectively (time interval is 3 h). The X-mark is the distribution of the buoy stations.

203 ous that NSD decreases with increasing intensity of hurricanes at location A (Fig. 8a) and at location B  
 204 (Fig. 8b). The results imply that the relative effect of the hurricane translation speed on waves decreases with  
 205 increasing intensity of the hurricane. The percentage of increase at the front-right location of hurricanes is  
 206 reduced and meanwhile the percentage of decreasing at rear-left of hurricanes increased. In other words, its  
 207 impact on the asymmetry of the wave field decreases with increasing intensity of the hurricane.

208 The mechanism used in Section 4.1 can also be applied here to explain this phenomenon. The influence of  
 209 hurricane translation speed on waves is mainly due to the possibility of interaction (resonance) between local  
 210 wind-generated waves and swells induced by past wind. Stronger winds (intense hurricane) will result in higher  
 211 peak wave periods, and higher group velocities. So for a given sub-critical hurricane translation speed, more  
 212 intense hurricanes are further from the resonance condition. The relative effect of swells would be less impor-  
 213 tant under an intense hurricane than under the situation of a weak hurricane.

214 4.4. The effect of hurricane wind distribution on waves

215 Actual hurricanes in nature are usually not symmetric in either wind speed or shape. In all previous exper-  
 216 iments (A, B, C), symmetric hurricanes are used. In this subsection, the effect of an asymmetric hurricane wind  
 217 field on hurricane-induced wave field will be examined. It is important to quantify the effect of wind asymme-  
 218 try on surface wind waves in order to provide either a justification for the current practice of using symmetric  
 219 hurricane wind model for wave forecasting, or recommend the use of asymmetric wind models. To evaluate  
 220 the effects of wind asymmetry on waves, two hurricane wind models are employed to simulate Hurricane Bon-  
 221 nie's (1998) wind field. One is assumed to be symmetric, as simulated by the H1980, and the other to be asym-

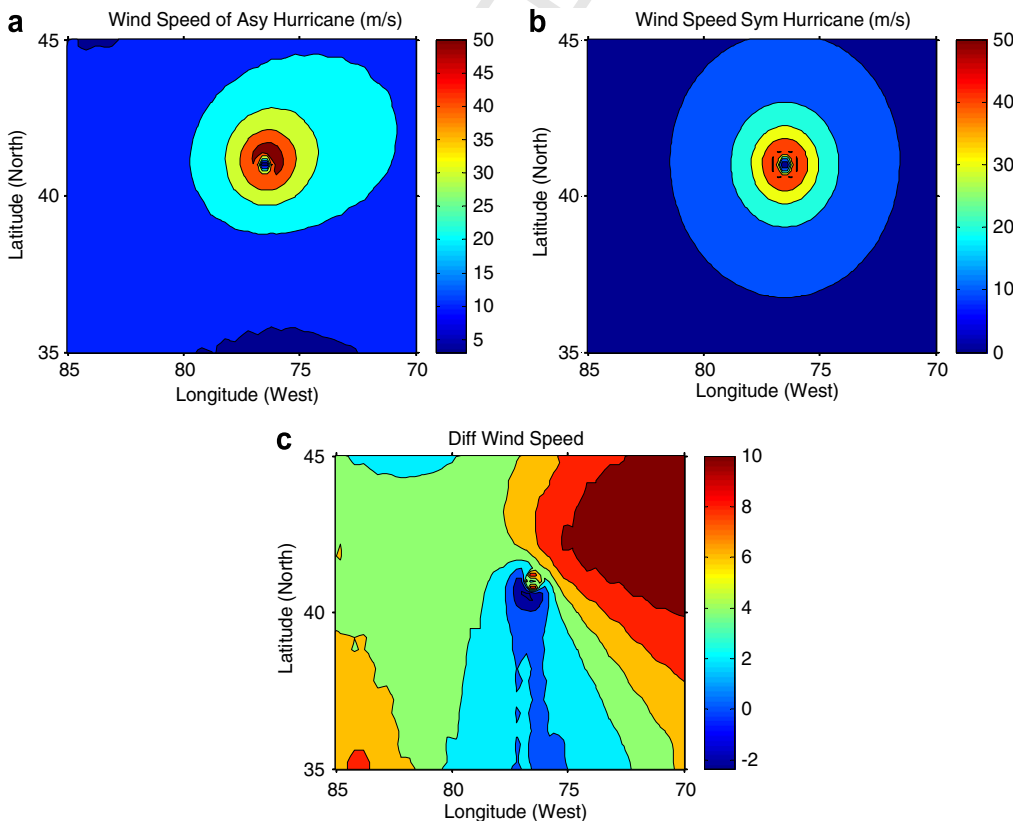


Fig. 10. (a) The distribution of symmetric hurricane wind fields (Bonnie) at 18:00 of Aug 25, 1998; (b) same as (a) but for asymmetric hurricane wind and (c) the difference between these two wind fields.

metric as simulated by HN2006. These simulations are referred to as Exp. D. The hurricane central pressure, translation speed and RMW are obtained from the NOAA “best track” database.

As Exp. D assumes an actual hurricane forcing, the domain is different from that used for the idealized cases in Exps. A, B, and C. Fig. 9 shows the model domain, extending latitudinally from 25° to 35° north and longitudinally from 85° to 70° west. Bottom topography is derived from the ETOP5 bathymetry database. The tracks of Bonnie and Floyd, which were used in the experiment, are also shown in Fig. 9 (time interval is 3 h). The track data is obtained from the NOAA “best track” database. Fig. 9 also shows the distribution of buoy stations, whose data was used to compare with the model results.

Fig. 10 displays the distribution of two hurricane wind fields and the difference between them at 18:00 of August 25, 1998 in the model domain. It is obvious that wind speeds to the front right of the hurricane track in the asymmetric hurricane are higher than those in the symmetric hurricane. Meanwhile, wind speeds to the rear left of the hurricane track in the asymmetric hurricane are weaker than those in the symmetric hurricane. Intuitively, this asymmetric wind speed distribution would cause the waves to be stronger in the front right areas and weaker in rear left areas than those generated by the symmetric hurricane. The distribution of SWH generated by these two hurricane wind fields and the difference between them are shown in Fig. 11a–c, respectively. It is apparent that the differences among them mainly appear in the front right and rear left quadrants. The SWH generated by the asymmetric hurricane are higher than that induced by the symmetric hurricane in front right areas, as expected. In contrast, the SWH are lower in the rear left areas, also as expected. These differences evidently reflect the asymmetry of the wind speeds. In other words, more wind speed asymmetry causes more asymmetric distribution of waves.

The above analysis clearly indicates the influence of asymmetric hurricane wind structure on waves. Presumably, the asymmetric hurricane wind model (HN2006) should produce more accurate wave forecasts.

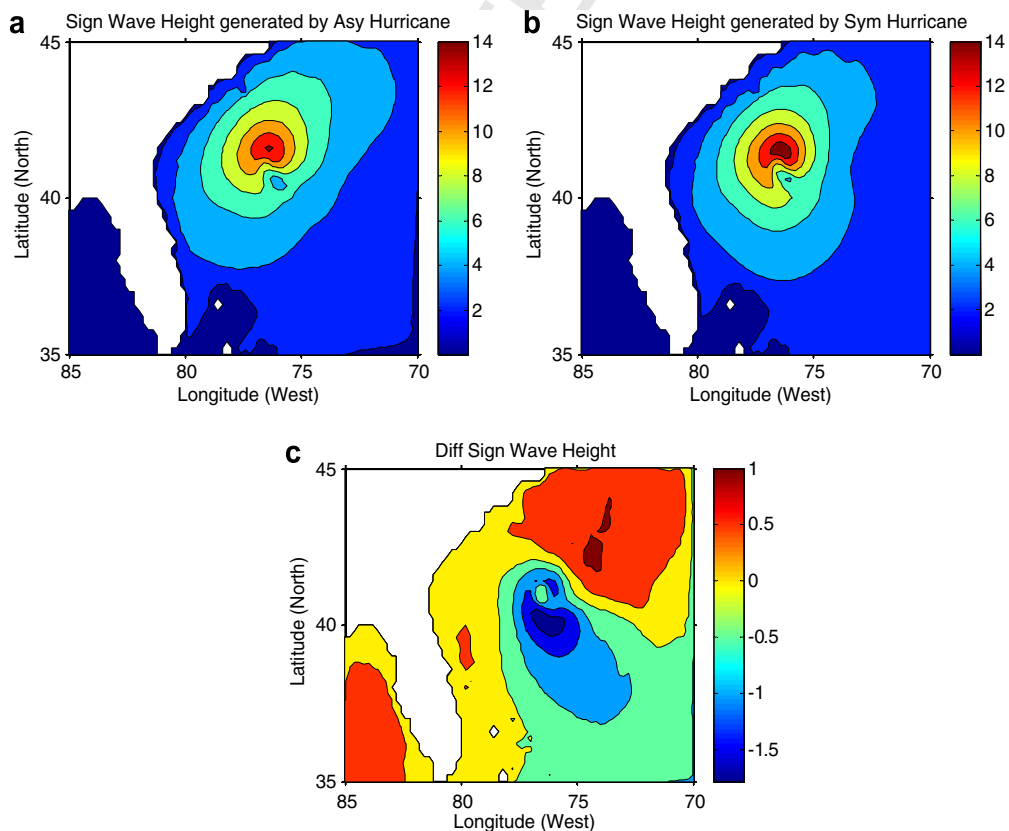


Fig. 11. (a) The distribution of SWH generated by symmetric hurricane wind (Bonnie) at 18:00 of Aug 25, 1998; (b) same as (a) but driven by asymmetric hurricane wind and (c) the difference between these two SWH fields.

244 To assess the performance of the wave model driven by the asymmetric, as opposed to the symmetric, hurri-  
 245 cane winds, the SWH generated by the two hurricane wind fields and the SWH obtained from the observa-  
 246 tional data at different buoy stations are compared (Fig. 12). The comparison shows that the SWH  
 247 generated by the asymmetric hurricane (HN2006) resembles more closely to the buoy data than do that gen-  
 248 erated by the symmetric hurricane (H1980) in most stations, especially at the Fpsn7 station (shown in Fig. 9),  
 249 which is located on the right side of Bonnie's track. The root mean square error (RMSE) of SWH generated by  
 250 HN2006 at three stations (41002, 41004 and Fpsn7) are 0.3182, 1.002 and 0.162 meters, respectively. As a com-  
 251 parison, the RMSE are 0.385, 1.146, and 0.6547 meters, respectively, in the H1980 case. The wind speed at  
 252 station Fpsn7 is stronger than that at a point the same distance to the left of Bonnie's track. The SWH sim-  
 253 ulated by the asymmetric wind field agrees very well with the observational data. Compared to the results from  
 254 the asymmetric wind model, the SWH produced by the symmetric wind field shows a much larger difference  
 255 from the observations taken at station Fpsn7, clearly indicating an under-prediction. However, compared to  
 256 the improvement of SWH simulation at station Fpsn7, the improvements at stations 41002 and 41004 are only  
 257 marginal. This may be due to the fact that stations 41002 and 41004 are located further away from the storm  
 258 than Fpsn7 (Fig. 9).

#### 259 4.5. The effect of background wind field on waves

260 In this subsection, the effect of background wind field on waves will be investigated by using hurricane  
 261 Floyd (1999) as an example. Two hurricane wind models are employed to simulate Hurricane Floyd's  
 262 (1999) winds. One is asymmetric as simulated by the HN2006 without incorporating the background wind

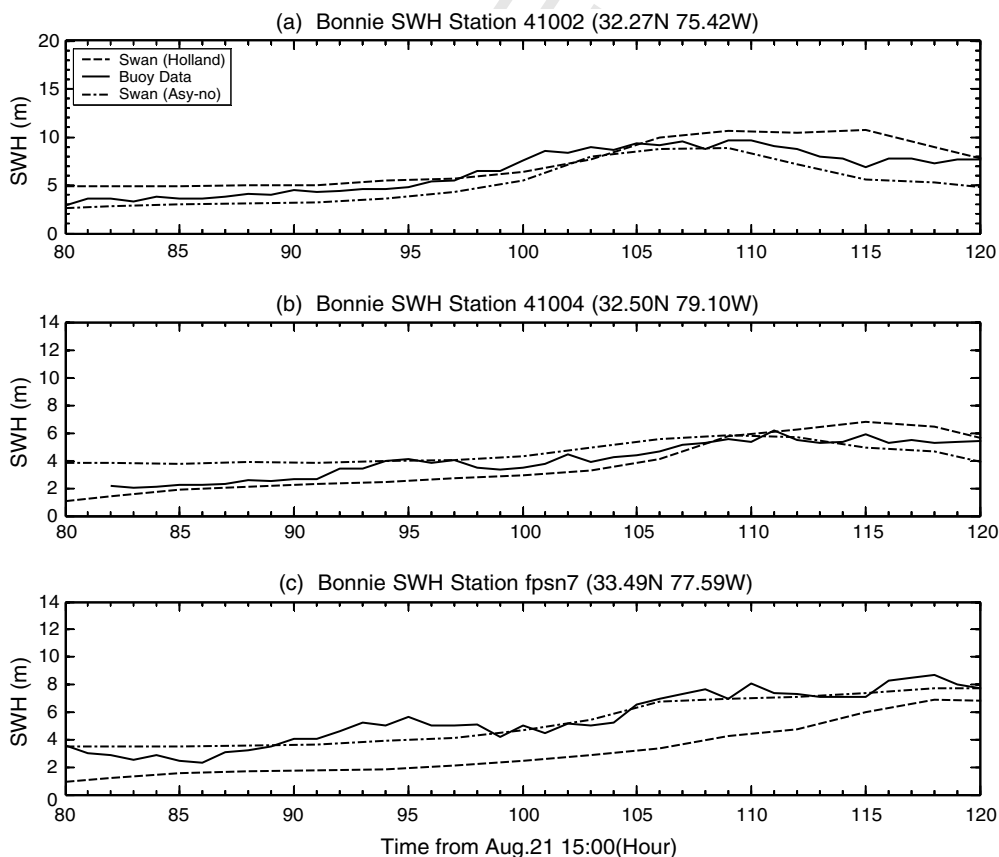


Fig. 12. SWH values during hurricane Bonnie at buoy station (a) 41,002; (b) 41,004 and (c) Fpsn7. Solid line is buoy data, dashed line is model results driven by symmetric hurricane and dot-dash line is model results driven by asymmetric hurricane wind.

263 field, and the other is asymmetric as simulated by HN2006, but also incorporates the background wind field.  
 264 The domain and settings of the parameters used in SWAN wave model are the same as in Section 4.4.

265 In general, parametric hurricane wind models such as H1980 or HN2006 do not include environmental  
 266 wind field. Thus, the simulated wind field will be zero before the front edge of a hurricane reaches the model  
 267 domain. The actual wind field, however, would not be zero even if the storm does not reach the domain  
 268 because of the presence of an environmental wind field. This phenomenon can be obviously seen from  
 269 Fig. 13. It shows the wind speed simulated by two hurricane wind models as compared to the observed wind  
 270 speeds at different buoy stations. The wind speed simulated by HN2006 without the background wind field is  
 271 almost zero at the beginning (Fig. 13), but the actual wind speed measured by the buoy is clearly not zero. The  
 272 waves driven by winds simulated by HN2006 without the background wind field is close to zero which is  
 273 clearly unrealistic before the storm winds enter the domain (Fig. 14). On the other hand, the wind speed mod-  
 274 eled by HN2006 with a merged background wind field is much closer to the observations during the early  
 275 hours (Fig. 13). The RMSE of wind speed simulated by HN2006 with a merged background wind field at three  
 276 stations (41004, 41008 and Fpsn7) are 1.044, 0.927 and 0.836 (m/s), respectively, during the first 24 h. As a  
 277 comparison, the RMSE are 1.205, 1.285, and 1.047 (m/s), respectively, in HN2006 without the background  
 278 wind field. Fig. 14 also shows the SWH generated by the two hurricane wind fields and the SWH obtained  
 279 from the observational data at different buoy stations. These figures show that the SWH produced by the  
 280 merged hurricane and background wind field (RMSE are 0.182, 0.226 and 0.199 m at stations 41004, 41008  
 281 and Fpsn7, respectively) is better than those generated by HN2006 alone (RMSE are 0.621, 0.304 and

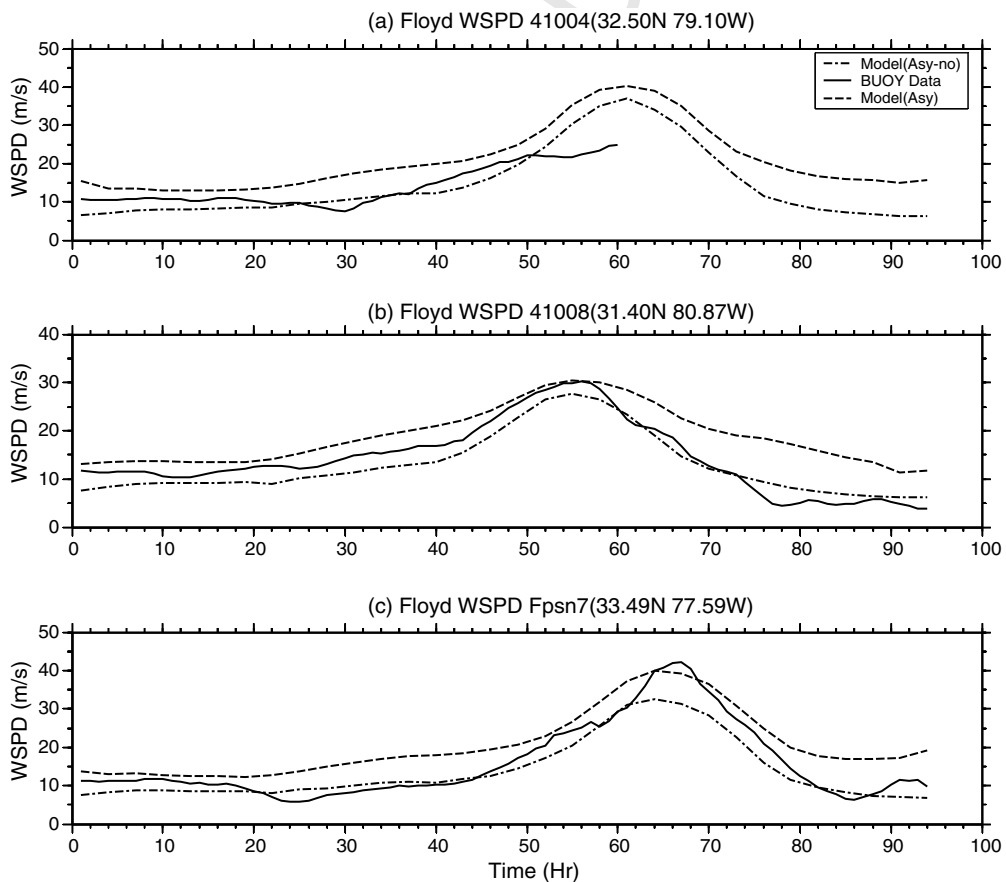


Fig. 13. Wind speed during hurricane Floyd at buoy station (a) 41,004; (b) 41,008 and (c) Fpsn7. Solid line is buoy data, dashed line is the result of asymmetric hurricane model including background wind field and dot-dashed line is the result of asymmetric hurricane model without background wind field.

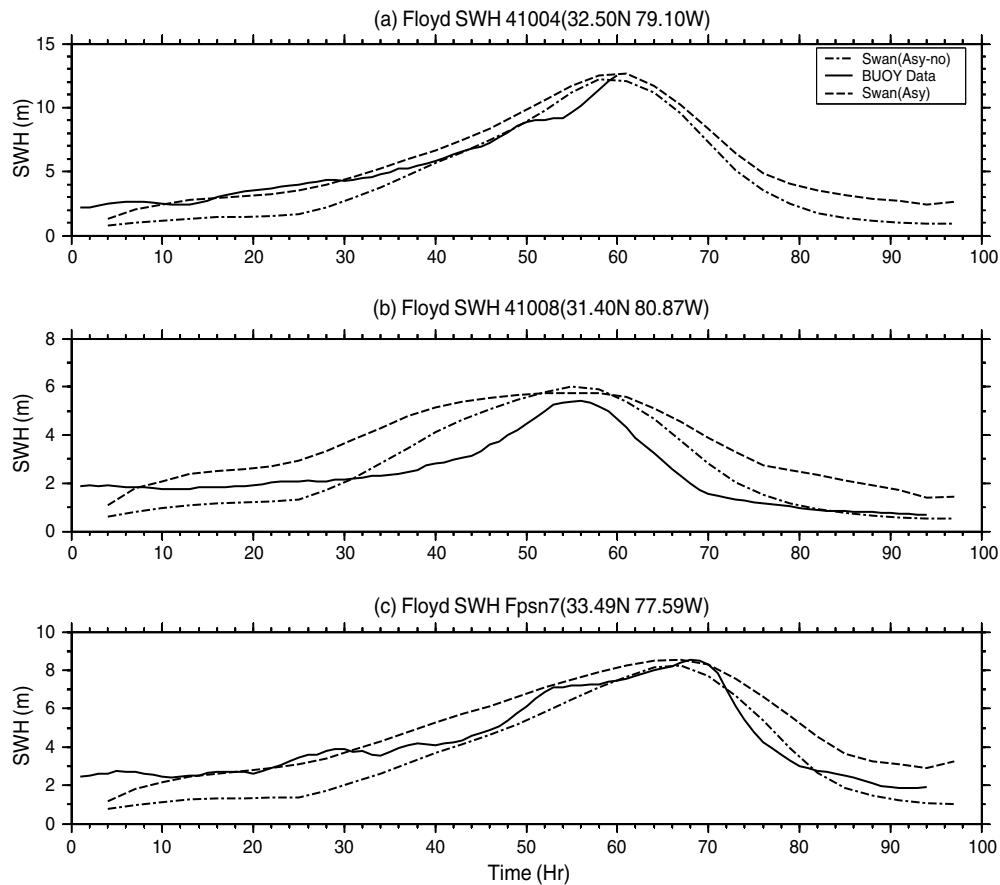


Fig. 14. Same as Fig. 13 but for SWH field.

282 0.575 m) during the first 24 h. It should be noted that, as seen from Fig. 13, including the background winds  
 283 improves the overall wind speed in the early hours, but not necessarily better than the stand-alone HN2006  
 284 after the storm's winds reaches the buoy, suggesting that whether or not including background winds is not  
 285 critical for the prediction of the peak waves produced by a storm.

## 286 5. Discussion and conclusions

287 In this study, the effect of hurricane wind distribution, translation speed, intensity, and background wind  
 288 field on sea surface wind waves was examined by using the SWAN wave model.

289 The results suggest that the hurricane translation speed makes a significant contribution to the asymmetric  
 290 structure of the waves. Furthermore, the translation speed can enhance of the SWH in the front-right quad-  
 291 rant of the hurricane track because of the resonance effect. This effect is significant when the hurricane trans-  
 292 lation speed increases to a value comparable to the group speed of the dominant waves; but small when the  
 293 hurricane translation speed is much larger or less than the group speed of the dominant waves. On the other  
 294 hand, the translation speed can reduce the value of the SWH in the rear-left quadrant of the hurricane track  
 295 because of a lessening of the wind forcing time and effective fetch. However, the waves may gain some energy  
 296 when the hurricane translation speed increases to the level that is comparable to the group speed of the dom-  
 297 inant waves.

298 The effect of hurricane intensity on waves is found to be such that SWH increases with increasing wind  
 299 speed. On the other hand, the hurricane translation speed causes less asymmetry for more intense hurricanes  
 300 than for weaker storms. Another factor affecting the structure of the wind waves is the asymmetric distribution

301 of hurricane winds. Considering the actual asymmetric structure of a hurricane can considerably alter the  
 302 SWH distribution produced by the hurricane and improve the skill of wind wave prediction. The effect of  
 303 background wind field on waves can be significant before the effect of hurricanes reaches the forecast domain.  
 304 Thus, the prediction of the wave SWH in the initial hours can be improved by merging the environmental  
 305 wind field into the hurricane wind field.

### 306 Acknowledgement

307 This study is supported by the Caroline Coastal Ocean Observation and Prediction System (Caro-Coops)  
 308 program, funded by the Coastal Services Center of the National Oceanic and Atmospheric Administration.

### 309 References

- 310 Booij, N., Ris, R.C., Holthuijsen, L.H., 1999. A third-generation wave model for coastal regions, 1. Model description and validation. *J.*  
 311 *Geophys. Res.* 104 (C4), 7649–7666.
- 312 Bowyer, P.J., MacAfee, A.W., 2000. The theory of trapped-fetch waves with tropical cyclones – an operational perspective. *Weather*  
 313 *Forecast.* 20, 229–244.
- 314 Hasselmann, K., Barnett, T.P., Bouws, E., Carlson, H., Cartwright, D.E., Enke, K., Ewing, J.A., Gienapp, H., Hasselmann, D.E.,  
 315 Kruseman, P., Meerburg, A., Müller, P., Olbers, D.J., Richter, K., Sell, W., Walden, H., 1973. Measurements of wind-wave growth  
 316 and swell decay during the Joint North Sea Wave Project (JONSWAP). *Dtsch. Hydrogr. Z. Suppl.* 12, A8.
- 317 Holland, G.J., 1980. An analytic model of the wind and pressure profiles in Hurricanes. *Mon. Wea. Rev.* 108, 121–1218.
- 318 King, D.B., Shemdin, O.H., 1978. Radar observations of hurricane wave directions, paper presented at 16th International Conference on  
 319 Coastal Engineering, Hamburg, Germany.
- 320 Komen, G.J., Cavaleri, L., Donelan, M., Hasselmann, K., Hasselmann, S., Janssen, P.A.E.M., 1994. *Dynamics and Modelling of Ocean*  
 321 *Waves.* Cambridge University Press, New York, 532 pp..
- 322 Kurihara, Y., Bender, M.A., Ross, R.J., 1993. An initialization scheme of hurricane models by vortex specification. *Mon. Wea. Rev.* 121,  
 323 2030–2045.
- 324 Miles, J.W., 1957. On the generation of surface waves by shear flows. *J. Fluid Mech.* 3, 185–204.
- 325 Moon, I.J., Ginis, I., Hara, T., Tolman, H.L., Wright, C.W., Walsh, E.J., 2003. Numerical simulation of sea surface directional wave  
 326 spectra under hurricane wind forcing. *J. Phys. Ocean.* 33, 1680–1760.
- 327 Moon, I.J., Ginis, I., Hara, T., 2004. Effect of surface waves on air-sea momentum exchange. Part II: behavior of drag coefficient under  
 328 tropical cyclones. *J. Atm. Sci.* 61, 2334–2348.
- 329 Ou, Shan-Hwei, Liau, Jian-Ming, Hsu, Tai-Wen, Tzang, Shiao-Yih, 2002. Simulating typhoon waves by SWAN wave model in coastal  
 330 waters of Taiwan. *Ocean Eng.* 29, 947–971.
- 331 Phillips, O.M., 1957. On the generation of waves by turbulent wind. *J. Fluid Mech.* 27, 4815–4827.
- 332 Ris, R.C., Holthuijsen, L.H., Booij, N., 1999. A third-generation wave model for coastal regions, 2. Verification. *J. Geophys. Res.* 104  
 333 (C4), 7667–7681.
- 334 Tolman, H.L., 1991. A third-generation model for wind waves on slowly varying, unsteady and inhomogeneous depths and currents. *J.*  
 335 *Phys. Oceanogr.* 21, 782–797.
- 336 Walsh, E.J., Wright, C.W., Vandemark, D., Krabil, W.B., Garcia, A.W., Houston, S.H., Murillo, S.T., Powell, M.D., Black, P.G., Marks,  
 337 F.D., 2002. Hurricane directional wave spectrum spatial variation at landfall. *J. Phys. Oceanogr.* 32, 1667–1684.
- 338 WAMDI Group, 1988. A third-generation model for wind waves on slowly varying, unsteady and inhomogeneous depths and currents.  
 339 *J. Phys. Oceanogr.* 21, 782–797.
- 340 Wang, D.W., Mitchell, D.A., Teague, W.J., Jarosz, E., Hulbert, M.S., 2005. Extreme waves under hurricane Ivan. *Science* 309, 896.
- 341 Wright, C.W., Walsh, E.J., Vandemark, D., Krabil, W.B., Garcia, A.W., Houston, S.H., Powell, M.D., Black, P.G., Marks, F.D., 2001.  
 342 Hurricane directional wave spectrum spatial variation in the open ocean. *J. Phys. Oceanogr.* 31, 2472–2488.
- 343 Xie, L., Wu, K., Pietrafesa, L.J., Zhang, C., 2001. A numerical study of wave-current interaction through surface and bottom stresses:  
 344 wind-driven circulation in the South Atlantic Bight under uniform winds. *J. Geophys. Res.* 106 (C8), 16841–16855.
- 345 Xie, L., Bao, S., Pietrafesa, L.J., Foley, K., Fuentes, M., 2006. A real-time hurricane surface wind forecasting model: formulation and  
 346 verification. *Mon. Wea. Rev.* 134, 1355–1370.
- 347 Young, I.R., 1988. Parametric hurricane wave prediction model. *J. Waterway Port Coastal Ocean Eng.* 114, 637–652.
- 348 Young, I.R., 2006. Directional spectra of hurricane wind waves. *J. Geophys. Res.* 111 (C8), C08020. doi:10.1029/2006JC003540.